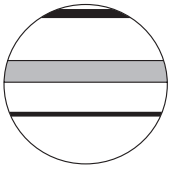

Research paper

The Holocene
1–9

DOI: 10.1177/0959683619831415
journals.sagepub.com/home/hol
SAGE

Onset of the African Humid Period by 13.9 kyr BP at Kabua Gorge, Turkana Basin, Kenya

Catherine C Beck,[1] Craig S Feibel,[2,3] James D Wright[2] and Richard A Mortlock[2]

Abstract

The shift toward wetter climatic conditions during the African Humid Period (AHP) transformed previously marginal habitats into environments conducive to human exploitation. The Turkana Basin provides critical evidence for a dynamic climate throughout the AHP (~15–5 kyr BP), as Lake Turkana rose ~100 m multiple times to overflow through an outlet to the Nile drainage system. New data from West Turkana outcrops of the late-Pleistocene to early-Holocene Galana Boi Formation complement and extend previously established lake-level curves. Three lacustrine highstand sequences, characterized by laminated silty clays with ostracods and molluscs, were identified and dated using AMS radiocarbon on molluscs and charcoal. This study records the earliest evidence from the Turkana Basin for the onset of AHP by at least 13.9 kyr BP. In addition, a depositional hiatus corresponds to the Younger Dryas (YD), reflecting the Turkana Basin's response to global climatic forcing. The record from Kabua Gorge holds additional significance as it characterized the time period leading up to Holocene climatic stability. This study contributes to the paleoclimatic context of the AHP and YD during which significant human adaptation and cultural change occurred.

Keywords

African humid period, Galana Boi, ostracods, paleoclimate, paleoenvironment, Turkana

Received 3 April 2017; revised manuscript accepted 23 December 2018

Introduction

East African climate

Climate variability has a major impact on environments and the ecosystems that depend upon it. The African Humid Period (AHP), spanning 15–5 kyr BP, is a significant event for East African climate (deMenocal et al., 2000; Shanahan et al., 2015; Tierney and deMenocal, 2013). Increased solar insolation because of Milankovitch forcing enhanced the intensity of the African monsoons, which simple climate models predict would have increased rainfall by 17–50% over the continent (Kutzbach and Liu, 1997). During the AHP, the typically endorheic Lake Turkana spilled into the Nile drainage basin through an outlet in the northwest of the present-day Omo River (Butzer et al., 1972; Garcin et al., 2012; Morrissey and Scholz, 2014). In contrast to the increased moisture of the AHP, the Younger Dryas (YD), a ~1-kyr cold interval in the northern hemisphere from 12.7 to 11.7 kyr BP (Rasmussen et al., 2006), corresponded to increased aridity in East Africa (Berke et al., 2014; Talbot et al., 2007). As a one of the largest catchments in the rift system, it is imperative to understand the timing and magnitude of base-level changes at Lake Turkana in response to the global climatic forcing like the AHP and the YD. These events have implications for resource availability for anatomically modern humans living in the basin and region (Shea and Hildebrand, 2010; Whitworth, 1965). In addition, understanding lake-level fluctuations through this time period provides an important analog for the Plio-Pleistocene record. The Turkana Basin preserves a long geological record (Feibel, 2011) with a rich fossil fauna assemblage, including many key hominin specimens (Wood and Leakey, 2011), the oldest stone tools described to date (Harmand et al., 2015), and evidence of early human warfare (Mirazon Lahr et al., 2016). Since much of the past 4 myr has been characterized by a high degree of climate variability (deMenocal, 1995), reconstructing the late-Pleistocene to Holocene paleoenvironmental response to paleoclimatic events in the basin informs broader interpretations of Plio-Pleistocene records such as the Hominin Sites and Paleolakes Drilling Project West Turkana Kaitio (HSPDP-WTK) core (Cohen et al., 2016).

Geologic setting

The Turkana Basin, located in the Eastern Branch of the East African Rift System (EARS) of northwestern Kenya and southern Ethiopia, contains sedimentary strata spanning more than 4 million years (Figure 1). Throughout the basin's history, lacustrine systems have waxed and waned due to the combined influences of tectonics and climate (Feibel, 2011). The Galana Boi Formation records the most recent phase of sedimentation in the Turkana Basin. The outcrop stratigraphy of the Galana Boi Formation was

[1]Geosciences Department, Hamilton College, USA
[2]Department of Earth and Planetary Sciences, Rutgers University, USA
[3]Department of Anthropology, Rutgers University, USA

Corresponding author:
Catherine C Beck, Geosciences Department, Hamilton College, 198 College Hill Road, Clinton, NY 13323, USA.
Email: ccbeck@hamilton.edu

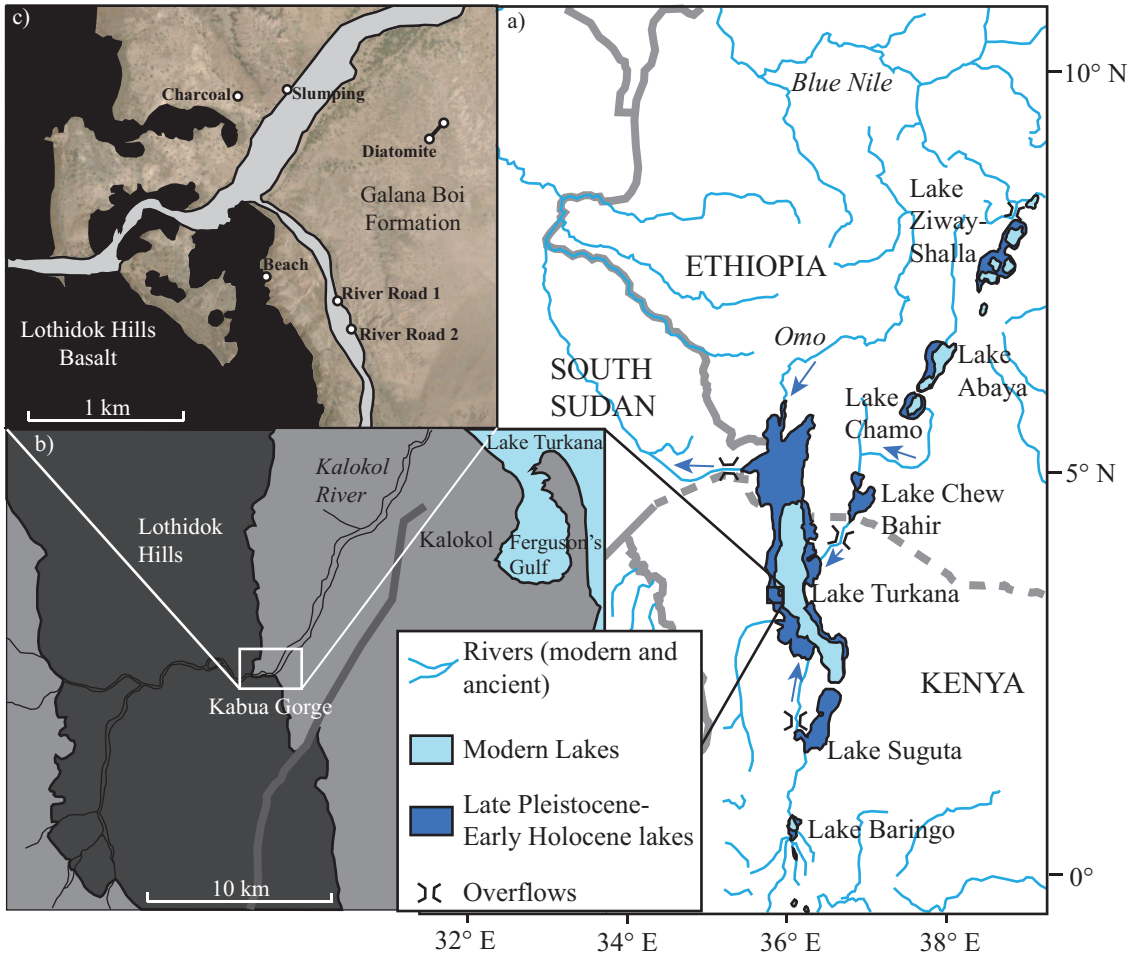

Figure 1. (a) Lakes of the Kenyan and Ethiopian parts of the EARS, highlighting hydrologic connections between basins in the past. (b) Map of the Kalokol region, the Lothidok Hills basalt (dark gray), and Kabua Gorge showing, (c) locations where stratigraphic sections were measured, outcrops investigated, and other significant samples were taken. The basalts of the Lothidok Hills are indicated in black and the channel of the modern Kalokol River is shaded in gray for emphasis; Figure 1a is modified from Garcin et al. (2012).

first described from the eastern margin of Lake Turkana by Vondra et al. (1971) and further developed by others (Harvey and Grove, 1982; Owen et al., 1982). The Galana Boi Beds, as they were originally called, were later promoted to formation status (Owen and Renaut, 1986); however, no type section was defined due to the spatial variability of these deposits and the badland topography which limits the availability of long, continuous sections (Owen and Renaut, 1986). In the type locality on the eastern side of Lake Turkana, the Galana Boi Formation is characterized by diatomaceous clayey silts that contain horizontal to wispy laminations and cross-bedded quartzofeldspathic sands.

Kabua Gorge is positioned to the west of Lake Turkana, ~12 km southwest of the town of Kalokol (Figure 1). The locality is ideally situated at an elevation to record deposition during highstand events. In this location, the Kalokol River forms a gorge through Miocene volcanics of the Lothidok Hills (Whitworth, 1965). Late-Pleistocene to Holocene sediments of the Galana Boi Formation rest unconformably on Pliocene Lonyumum Member deposits of the Nachukui Formation or directly on Miocene volcanics. Based on field observations and mapping, the Galana Boi section at Kabua Gorge is not rotated and there are no faults with significant offset (>1 m) in the study area. Extensive investigation of the Galana Boi Formation and the laterally equivalent Member IV of the Kibbish Formation in southern Ethiopia (Brown and Fuller, 2008) found no evidence of significant faulting in these strata. While the Turkana Basin remains tectonically active and flexural rebound occurs in volcanically active areas in the center of the basin such as South Turkana and the Suguta Basin to the south (Melnick et al., 2012), much of the Turkana Basin has remained tectonically quiescent over the past 200,000 years when subsidence was concentrated in the center of the basin (Feibel, 2011).

Methods

Fieldwork

Fieldwork conducted in the summers of 2011–2015 at Kabua Gorge focused on the following activities: (1) measuring sections through the Galana Boi Formation to facilitate comparisons with other Holocene sedimentary archives from cores and outcrops; (2) mapping outcrops in the environs of Kabua Gorge to provide a spatial, as well as temporal, setting for deposition; and (3) collecting bulk sediment samples for subsequent analyses, including AMS radiocarbon dating and isotopic analysis ($\delta^{13}C$ and $\delta^{18}O$) of ostracods.

Radiocarbon dating

Six AMS radiocarbon dates were generated from the sections, four from molluscs (*Melanoides tuberculata*) and two from charcoal. Three shell dates came from the base of each of the lacustrine intervals at River Road 1 (RR1) (Figure 1). A fourth shell date came from a smaller exposure 1.58 km north of RR1 (Charcoal section) and allowed for a paired charcoal–mollusc date to estimate potential reservoir effects. ^{14}C ages are reported in calibrated years before present (cal yr BP) using the IntCal13 database.

Table 1. AMS radiocarbon dates from Kabua Gorge.

Lab ID (beta)	Location	Material	$\delta^{13}C$ (‰)	Conventional ^{14}C dates (BP)	2-sigma calibrated result (cal yr BP)	Median age (cal yr BP)	Elevation (m)
402648	Charcoal section	Charcoal	–26	9390 +/– 30	10695–10560	10630	420
402649	Charcoal section <4 cm below charcoal	Mollusc	–3.3	9640 +/– 30	11175–11070, 10955–10865, 10850–10805	10990	420
3775179	Slumping section	Charcoal	–24.4	9540 +/– 40	11085–10920, 10890–10705	10900	418
396299	River Road 1	Mollusc	–4.1	10130 +/– 40	11970–11610, 11520–11510	11740	445
396300	River Road 1	Mollusc	–2.4	11160 +/– 40	13090–12990	13040	442
396301	River Road 1	Mollusc	–4.4	12010 +/– 40	13980–13755	13870	438

All measurements were made at Beta Analytic Radiocarbon Dating; conventional C14 ages are converted to calendar age using Calib 7.1 (IntCal13) and reported uncertainties represent 2-sigma (68% probability). In cases with bimodal or trimodal distributions, the median age was used. No reservoir age correction is applied to dates and all elevations are reported as recorded in the field using GPS.

Ostracod analysis

Approximately, 1 cm^3 of sample material was weighed and soaked in distilled water to disaggregate the sediment. Samples went through multiple wet–dry cycles until the ostracods could be separated from the clay by wet sieving on a 120 mesh (125 μm) screen with distilled water. The remaining material was studied under a binocular microscope, noting clast composition, presence of organics, and fish remains (teeth, scales, and bones). The ostracods were identified to the genus level based on comparison with previous studies (Carbonel and Peypouquet, 1979; Cohen, 1986; Feibel, 1988).

Stable isotopes

Measurements of $\delta^{13}C$ and $\delta^{18}O$ were made on ostracod valves using a Fisons Optima mass spectrometer equipped with a Micromass MultiPrep automatic sample processing system in the Stable Isotope Lab at Rutgers University. Each stable isotope measurement ($\delta^{13}C$ and $\delta^{18}O$) was performed on 6–10 individual valves of *Limnocythere* sp. Replicates of selected samples were run to check for reproducibility of results. Ratios are reported in standard delta notation in parts per thousand (per mil, ‰) $\delta = ((R_{sample}/R_{standard}) - 1) \times 1000$ where $R = {}^{13}C/{}^{12}C$ or ${}^{18}O/{}^{16}O$, relative to Vienna-Pee Dee Belemnite ($\delta^{13}C$ and $\delta^{18}O_{VPDB}$) through the analysis of an in-house laboratory standard (RGF1) calibrated to NBS-19 to ensure consistency in reported values. Analytical error (1-sigma) is ± 0.05‰ and ± 0.08‰ for $\delta^{13}C$ and $\delta^{18}O$, respectively, based on replicate analyses of the in-house standard.

Results and discussion

Chronology

Mollusc (*M. tuberculata)* and charcoal ^{14}C ages provide the chronologic framework for the stratigraphy (Table 1). However, because the sand units between fine-grained phases represent unknown interval of time, a continuous age model could not be constructed. In addition to providing chronology, this study tested the assumption that the reservoir correction at Lake Turkana is negligible (Berke et al., 2012; Garcin et al., 2012; Halfman et al., 1994; Morrissey and Scholz, 2014; Owen et al., 1982). A stratigraphically contemporaneous mollusc (ID 402649; 9640 +/– 30 BP) and charcoal pair (ID 402648; 9390 +/– 30 BP) from the Charcoal section showed a 250 ^{14}C-year offset. This is the first quantification of a reservoir effect in Turkana. While our data show that a small, but measurable, reservoir effect exists, we did not apply a reservoir correction to radiocarbon ages prior to converting to calendar ages in order to facilitate direct comparison between this study and previous work. Further research is needed to determine if this age offset is a function of local fluvial input introducing older carbon to the system or represents a basin-wide reservoir effect that should be systematically corrected.

Stratigraphy

The stratigraphy presented here is based on the River Road 1 (RR1) section (Figure 2) but includes observations and lateral facies relationships established through investigation and comparison with other sections measured at Kabua Gorge. The section is characterized by three laminated intervals separated from one another by fine-grained sand units. Across the study area, these intervals varied subtly, with some sections characterized by wispy diatomaceous laminae and others dominated by gray silts. These laminated intervals represent lacustrine deposition and will subsequently be referred to from oldest to youngest as Phases 1, 2, and 3. The base of each lacustrine Phase was dated using radiocarbon analyses performed on mollusc shells. An additional lacustrine or lagoonal interval, corresponding to black, organic-rich clays, was identified above Phase 3. It is not included in this study because of the degree to which it differs sedimentologically from underlying intervals. In addition, ostracod preservation in this uppermost lacustrine unit was poor relative to Phases 1–3 and therefore isotopic analysis on a comparable scale was not possible. To the west, paleoshoreline and beach deposits are preserved lapping onto the Lothidok Basalts. The beach facies comprised fine to coarse sands, with intervening beds of poorly sorted pebble conglomerates that are interpreted to represent paleobeaches. Due to the potential reoccupation and reworking of these paleoshoreline deposits by multiple highstand events, these surfaces were not stratigraphically tied to any particular lacustrine interval.

The RR1 section lies unconformably upon well-lithified, altered sediments from the Pliocene Lonyumum Member of the Nachukui Formation, represented by a coquina of recrystallized *Cleopatra bulimoides* overlain by gravel to caliche gravel. The Galana Boi section begins with 1.1 m of medium to coarse, well-sorted lithic sand with trough cross-beds. The next overlying unit is 1.6 m thick and consists of fine to medium well-sorted lithic sand with discrete planar beds of heavy mineral concentrated black sands. Planar cross-beds are visible in the upper ~10 cm of this interval. The upper contact is irregular and marked by a concentration of mollusc shells.

Above this contact, the first fine-grained interval of lacustrine deposition (Phase 1) occurs, as indicated by 3.0 m of laminated to planar-bedded silty clay. The unit contains sparse *M. tuberculata* shells, charcoal fragments, and ostracods. The clays of Phase 1 are overlain by 0.8 m of silty sand, with trough cross-beds and distinct silt lenses. *M. tuberculata* shells are abundant in isolated, discontinuous beds and ostracods are present. Phase 2 is sedimentologically similar to Phase 1, 2.8 m thick, and again it is overlain by another 0.6 m of the silty sand facies. Phase 3 is similar in character to the lower two silty clays but is thinner (1.4 m). This

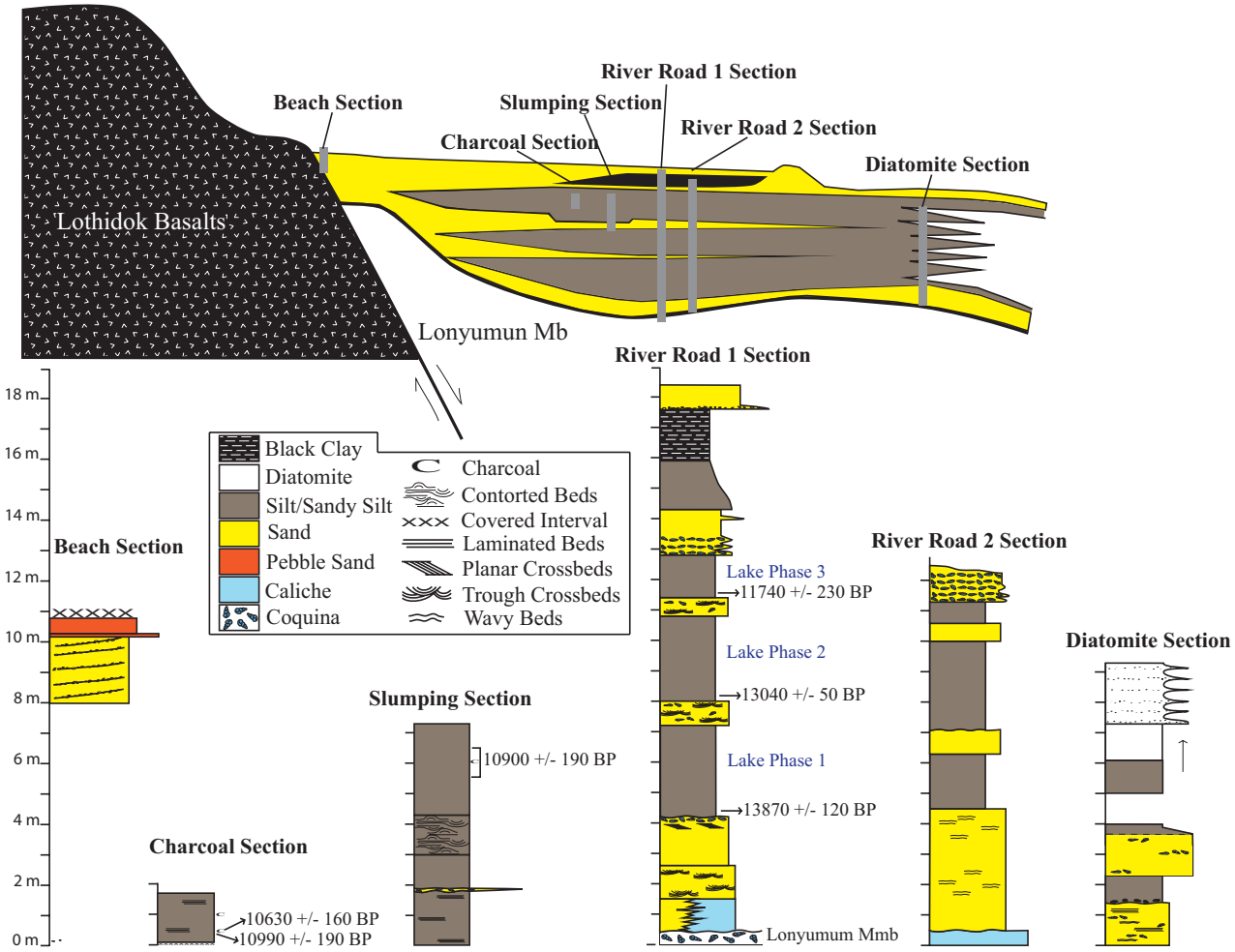

Figure 2. Facies model showing schematic representation of the lateral and temporal relationships between stratigraphic sections measured from outcrops at Kabua Gorge. While the true thickness of the sections is indicated, their elevations and lateral spacing are not to scale. Stratigraphic positions of ages obtained from radiometric dating (Table 1) are shown to the right of the columns. The map-view positions for each named section are indicated on Figure 1.

silty clay facies was laterally extensive in the study area and likely correlates to sediments in the River Road 2, Charcoal, and Slumping sections. Phase 3 is capped by a series of coquina beds in an overall silty sand unit (1.1 m) with isolated coarser sand lenses. The next unit is 1.6 m of fine sand grading up section to silt with prevalent shell beds dominated by the *Corbicula consobrina*, although *M. tuberculata, Mutela nilotica*, and *Caelatura (Nitia) monceti* are also present. The upper contact is a gradational one that has been assigned primarily on the basis of color, as the clayey silt fines to black clay. The black clay unit is 1.7 m thick. There are strong lithologic and biological indicators that the black clay unit represents sedimentation in a fluctuating wetland environment. It has a high percentage of organic carbon (~6%) and contains botryoidal pyrite, the first documented in outcrop from the Turkana Basin (Figure 3m–n), both of which suggest a reducing environment. Further evidence of the dynamic nature of this marginal environment comes from pedogenesis throughout the black clay, indicating that the area was repeatedly subaerially exposed for long intervals such that soils could develop. Finally, biological evidence comes from the presence of *Pila ovata*, an aquatic pulmonate mollusc that prefers swampy conditions (Brown, 1980) and is found in the section along with lacustrine molluscs (*M. tuberculata, M. nilotica, C. consobrina, Etheria elliptica*). This assemblage suggests that Kabua Gorge was a dynamic, fluctuating margin that was sometimes subaerial and sometimes subaqueous, potentially on a seasonal basis. The upper contact of the black clay is irregular and the overlying unit has a basal pebble lag. This unit is approximately 0.8 m thick and comprises fine to medium, well-sorted lithic to mafic rich sand that is interpreted to represent a beach surface and the cessation of lacustrine deposition at Kabua Gorge.

Ostracod assemblages and interpretation

Six genera of ostracods, with both adults and juveniles, were identified in the Galana Boi Formation at Kabua Gorge (Figure 3; see Supplement for full dataset, available online). The ostracod assemblages in the three lacustrine phases of the RR1 section are distinct from one another on the basis of key genera presence/absence (Figure 4). The section is dominated by juvenile specimens, which are the basis for the discussion that follows. The juvenile data are presented here as the large numbers of individuals increase the significance of the trends presented. The abundance of juveniles also supports the interpretation that this is a life assemblage, as opposed of a taphonomic concentration of valves after the organisms die (Zhai et al., 2014).

Phase 1 has the lowest overall ostracod abundances of the three lacustrine phases, with a maximum concentration of ~581 juvenile valves per gram of sediment. The base of the Phase 1 interval (samples 22 and 22.5) has a low abundance, *Limnocythere* sp. dominated assemblage. The middle of Phase 1 (23) increases in total abundance, and the ostracod *Darwinula* sp. dominates the

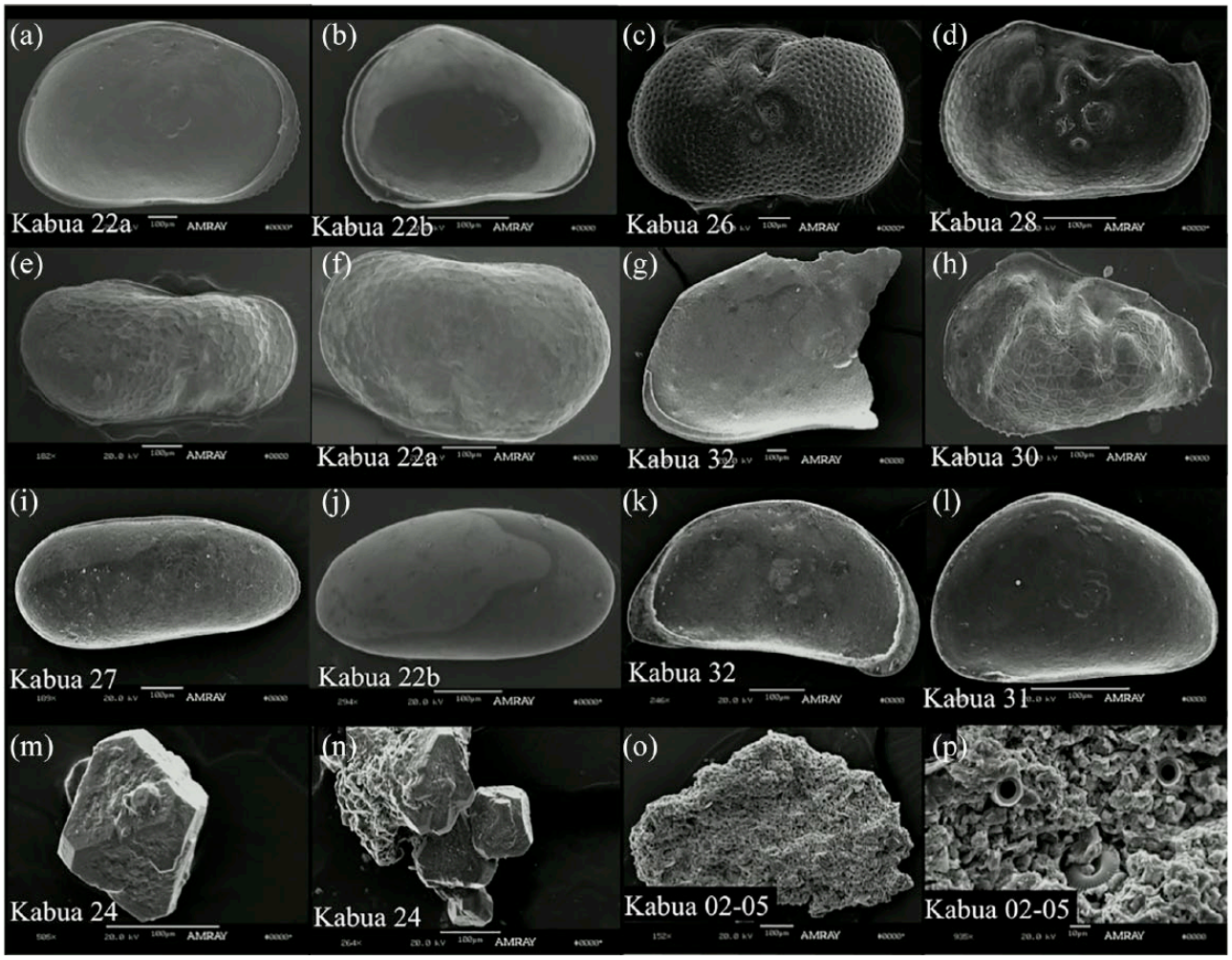

Figure 3. SEM images of the main ostracod taxa and other biologic remains found in the Kabua Gorge RR1 section: (a) *Hemicypris* sp. adult; (b) *Hemicypris* sp. juvenile/Species X; (c) *Ilyocypris* sp. adult; (d) *Ilyocypris* sp. juvenile; (e) *Limnocythere* sp. adult; (f) *Limnocythere* sp. juvenile; (g) *Sclerocypris* sp. adult fragment showing characteristic posterior angulation; (h) *Sclerocypris* sp. juvenile with earliest instar morphology; (i) *Darwinula* sp. adult; (j) *Darwinula* sp. juvenile; (k) *Potamocypris* sp. adult; (l) *Potamocypris* sp. juvenile; (m) single pyrite framboid; (n) cluster of pyrite framboids held together which crusty, white material; (o) large piece of vegetation; (p) zoomed in image of (o) showing stomata-like features with high degree of preservation.

assemblage. The top of Phase 1 (24) has the most ostracods within this Phase, with a strongly *Darwinula* sp. dominated assemblage. Transitioning into the first sandy interval (25), the ostracod count drops dramatically, potentially due to the taphonomic processes mentioned above. One example is that the abundance of *Darwinula* sp., one of the most fragile ostracods in this assemblage, decreases significantly, while the more durable *Limnocythere* sp. valves are less impacted.

In Phase 2, *Limnocythere* sp. and *Darwinula* sp. remain dominant but are joined by *Ilyocypris* sp. at the base of the lacustrine interval (26). The middle and the top of this phase (27 and 28) are distinct because they mark the appearance of *Sclerocypris* sp. and a steady decline in *Limnocythere* sp. Again, the second sandy interval (29) has very low total ostracod abundances and the decline in *Limnocythere* sp. continues.

Phase 3 is dominated by *Darwinula* sp., with Species X (likely a juvenile *Hemicypris* sp.) as the second most abundant ostracod. In contrast to Phase 2, *Ilyocypris* sp. is extremely rare in this interval. While the total ostracod abundances are nearly as low at the base on the lacustrine interval (30) as they were in the second sand (29), the middle (31) and top (32) of this interval contain a unique assemblage. Like in Phase 2, *Sclerocypris* sp. also appears in this interval but in Phase 3 there is also abundant *Potamocypris* sp. which is not seen anywhere else in this Holocene section but is very abundant in the Common Era record from Ferguson's Gulf (Beck, 2015; Beck et al., 2014). Based on its abundance in the modern Ferguson's Gulf (Beck, 2015), *Potamocypris* sp. is interpreted to represent a protected, shallow, and highly productive lake marginal environment like a marsh or lagoon. This effect could be produced by spit formation such as exists in modern Ferguson's Gulf. Along the western shore of Lake Turkana, many sand 'beach' ridges have been identified (Martin, 2014). Potentially, these ridges might have played a role in protecting Kabua Gorge. Alternatively, this environment may have been isolated by local topographic highs, like Sanderson's Gulf in the northwestern corner of the modern lake, creating a protected embayment.

Isotopic interpretation

Results from isotopic analysis of $\delta^{13}C$ and $\delta^{18}O$ on Kabua Gorge ostracods are shown in Figure 4. The data for both $\delta^{13}C$ and $\delta^{18}O$ are plotted versus sample elevation from the corresponding RR1 section. Values range from −1.8 to 3.2‰ for $\delta^{13}C$ and −0.4 to 3.9‰ for $\delta^{18}O$. No significant trend in the $\delta^{13}C$ values is observed in the data, which may reflect the competing roles of bioproductivity, changes in the rate of exchange between pCO_2 and surface water, and riverine-lake end-member mixing (Ricketts and Anderson, 1998). Today, the pervasive wind of the Turkana Jet (Nicholson, 1996) maintains constant mixing and thereby promotes rapid exchange and equilibrium between atmospheric CO_2

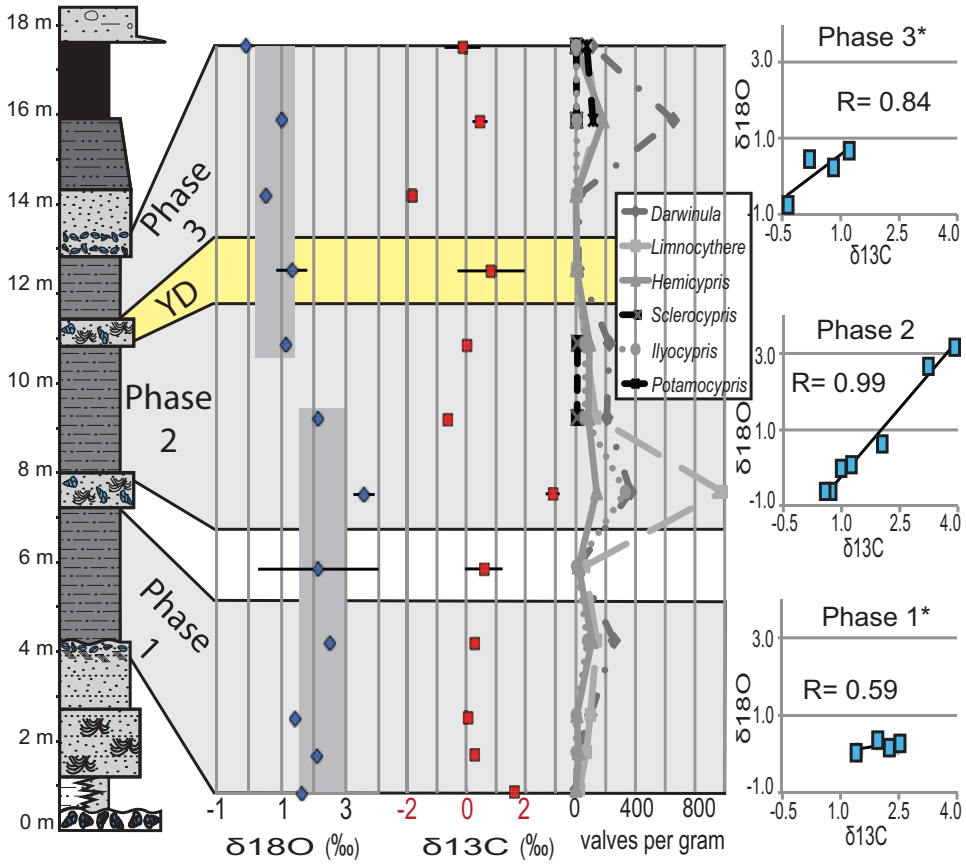

Figure 4. Results of isotopic analysis on *Limnocythere* sp. for $\delta^{13}C$ and $\delta^{18}O$ and ostracod juvenile taxa counts (in valves per gram) shown in the context of the stratigraphic section River Road 1.
The inferred YD (~12.8–11.6 kyr BP) is highlighted in yellow; gray boxes on $\delta^{18}O$ data show average of data points for interval and highlight isotopic shift in Phase 2, interpreted to signify a freshening of the system as overflow conditions were achieved; plots of $\delta^{13}C$ versus $\delta^{18}O$ are displayed for covariance calculations; see Supplemental Appendix (available online) for full ostracod data.

and $CO_{2[aq]}$ in the water column of Lake Turkana. If this system was more variable in the past and the lake developed some stratification, then the relationship could have broken down, complicating the interpretation of the $\delta^{13}C$ record.

In contrast, the $\delta^{18}O$ record of ostracod calcite ($\delta^{18}O_{cod\ calcite}$) shows a lowering of $\delta^{18}O$ of about 1.5‰, beginning in the middle of Phase 2 and continuing through Phase 3 of the record (Figure 4). Modern values of $\delta^{18}O_{water}$ (6‰) and $\delta^{18}O_{cod\ calcite}$ (3.5‰) suggest calcification temperatures of 27–28°C (Vonhof et al., 2013) and are consistent with observed annual temperature range of 26–30°C for modern Lake Turkana surface water (Berke et al., 2012). The observed scatter in the paleorecord (range of 1.5‰) is also consistent with the range in modern ostracods and attributed to varying riverine input to Lake Turkana (Vonhof et al., 2013). Mean $\delta^{18}O_{cod\ calcite}$ of 2.3‰ prior to the Phase 2 shift suggests $\delta^{18}O_{water}$ of about 4.5‰ (O'Neil et al., 1969) assuming lake temperature was similar to the modern, an observation supported by the lake's equatorial position and extremely limited seasonal variability. We suggest that the lowering of $\delta^{18}O_{cod\ calcite}$ by 1.5‰ during Phase 2 represents lower $\delta^{18}O_{water}$ during a lake-wide freshening event preceding the YD lowstand. This freshening event is likely tied to Lake Turkana reaching overflow conditions. Garcin et al. (2012) documented overflow beginning around 11.7 kyr BP, or Phase 3 of this study. However, our isotopic data suggest that there is a previously unrecognized overflow event closer to ~13 kyr BP during Phase 2 (Figure 5a). We suggest that this earlier highstand event might not be distinguishable from subsequent ones of the same elevation because of reoccupation of the paleo-shorelines presented by Garcin et al. (2012). In addition, a pre-13 kyr BP response to AHP moisture in the Turkana Basin was suggested from two AMS radiocarbon dates from *Melanoides* presented in Bloszies et al. (2015). This study builds upon these records to further refine the oldest part of Turkana Basin's response to the AHP.

While absolute values of $\delta^{13}C$ and $\delta^{18}O$ have been shown to be unreliable indicators of lake level in the Turkana Basin (Ricketts and Anderson, 1998), the covariant relationships between the $\delta^{13}C$ and $\delta^{18}O$, as developed for closed basin systems by Li and Ku (1997), further support this lake-level reconstruction (Figure 4). During Phase 1, covariance is relatively poor ($R = 0.59$) even after removing one outlier point from the base of the section from the regression. This data point is enriched in both $\delta^{13}C$ and $\delta^{18}O$ and potentially represents the early stages of the lake transgression in this area. Conversely, Phase 2 has very high covariance ($R = 0.99$). Li and Ku (1997) attribute this kind of isotopic relationship to a system that never stabilized, potentially because it underwent a rapid transgression. The presence of *Sclerocypris* sp. also suggests that the lake was deeper toward the middle to top of Phase 2. Covariance again breaks down in Phase 3 ($R = 0.41$), although removal of one outlier point brings it up ($R = 0.84$) (Figure 4). This is primarily attributed to a shift in $\delta^{18}O$ toward lower values. In the broader paleolimnologic context, this transgression marks a well-documented event when Holocene Lake Turkana achieved overflow conditions at an elevation of ~ 460 m and spilled into the Nile drainage basin. However, the freshening of Lake Turkana at first seems slightly at odds with the presence of *Potamocypris*, which usually indicates restricted, shallow environments. However, because the base of Phase 3 occurs at an elevation of 438 m (Table 1), the maximum water depth during overflow for this sedimentary package was only 22 m. Therefore,

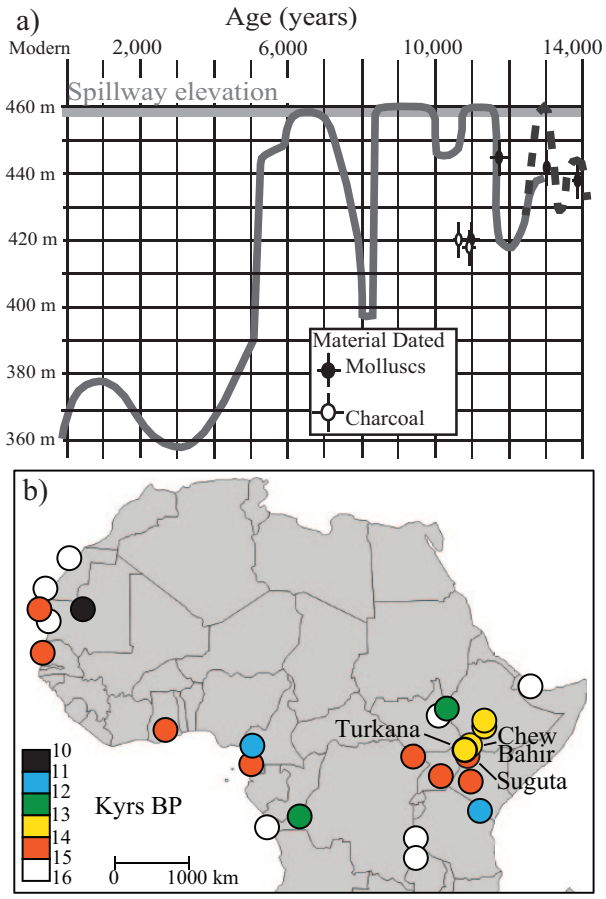

Figure 5. (a) Late-Pleistocene to Holocene lake-level record (Garcin et al., 2012) for Lake Turkana as refined by this study. Garcin et al. (2012) was chosen as the base record for this reconstruction because it represents the most comprehensive recent lake-level curve compilation and contains the data that is most relevent for this discussion. Dashed line is modification of curve based on this study, which extends the record of the response to the AHP back to nearly 14 kyr BP. In addition, outcrop work was able to increase the resolution of this record and add a previously undocumented lowstand around 13 kyr BP on the basis of beach/littoral facies. (b) Map showing timing of onset of AHP across the African continent. Figure modified from Shanahan et al. (2015) to include the record from Lake Turkana's onset (position noted with a T) by 13.9 kyr BP, as documented by this study. Paleo-Lake Suguta (Junginger et al., 2014) and Chew Bahir (Foerster et al., 2015) have also been added to this compilation.

the *Potamocypris* likely inhabited a relatively shallow, littoral zone, and their presence is due to the local paleoenvironmental setting as opposed to the freshness of the whole lake. This suggests that either the accommodation space in the Turkana Basin filled, leading to a shallower lake despite wetter conditions and a lacustrine highstand, or coastline geometry formed a protected, marshy bay in the area around Kabua Gorge.

Regional synthesis

The onset of the AHP response in Lake Turkana follows the cessation of Heinrich 1 (15 kyr BP), which has been correlated to megadroughts across the Afro-Asian monsoon region (Stager et al., 2011) and West Africa (Shanahan et al., 2015). Strong evidence from paleo-Lake Suguta highlights the complexity of precipitation sourcing across East Africa as it appears likely that a northward shift in the Congo Air Boundary (CAB) and increased East Asian monsoon activity initiating at 14.8 kyr BP also played an important role in the AHP (Junginger et al., 2014). No new mechanism is needed to explain the onset of the AHP close to 14 kyr BP in the Turkana Basin. It is synchronous with records from Ethiopia that are proximal to the headwaters of the Omo River. Today, the Omo contributes anywhere from 80% to 90% of the water to Lake Turkana (Yuretich and Cerling, 1983). Therefore, even if local rivers were contributing more water to the lake, the Omo River likely remained the primary input to the hydrologic budget of Lake Turkana. On a regional scale, Lake Turkana's AHP response is coeval with both Chew Bahir (Foerster et al., 2012) and paleo-Lake Suguta (Garcin et al., 2014; Junginger et al., 2014) basins to the north and south that were hydrologically connected (van der Lubbe et al., 2017) (Figure 5b). This suggests that this section of the EARS was simultaneously responding to the broader regional climatic forcing. Work from paleo-Lake Suguta, including hydrological modeling, demonstrated that the AHP lake-level rise could only be achieved by an abrupt increase of between 26% and 40% in precipitation around 14.8 kyr BP (Junginger and Trauth, 2013). Since the timing of the onset of the AHP is similar between the Suguta and Turkana, then the simplest explanation for this synchronicity is that the mechanism driving the lake-level rise was also similar. This suggests that Lake Turkana also experienced a rapid onset to the AHP.

Like the asynchronous termination of the AHP, which occurred progressively later at lower latitudes (Shanahan et al., 2015), the onset of the AHP recorded in the Turkana Basin supports an asynchronous spatial trend across the continent. In part, this might be a function of the limited number of paleorecords preserving the onset of wetter conditions. The record from Kabua Gorge fills a significant gap in the understanding of the paleoclimatic response to the AHP in the Eastern Branch of the EARS by connecting records from the Ethiopian Highlands to those from central Kenya. The data from Turkana put the basin's first AHP highstand on the threshold between the record from southern Kenya/Tanzania (Lake Challa) at 15–14 kyr BP (Tierney et al., 2011) and those from Ethiopia at 14–13 kyr BP (Shanahan et al., 2015; Street-Perrott and Perrott, 1990). This suggests a trend, at least within the Eastern Branch, of an earlier onset of the AHP in Kenya and later in the higher latitudes (Figure 5b). However, further study is essential to evaluate the extent of this potential trend. The asynchronicity of the onset of the AHP might be a function of local, basin-scale sensitivity to the increased insolation of the AHP. Heterogeneity characterizes other Holocene climatic events preserved in continental records such as the 'Little Ice Age' (Russell et al., 2007). While the mechanisms controlling this may not yet be clear, it is reasonable to assume that as the resolution of paleorecords increases and expands the understanding of AHP, we may observe asynchronous timing. On human time scales, this is important as it allows for populations to leverage resources across the landscape by migrating to refugia. Coastal regions of Lake Turkana have been proposed as refugia during short, dry events such as the YD (Foerster et al., 2015). Further research is needed to determine the paleoenvironmental consequences of these paleoclimatic events.

Conclusion

This study increases the resolution of the late Pleistocene to early Holocene lake-level curve for Lake Turkana by defining and refining three distinct deep-water lacustrine phases beginning by at least 13.9, 13.0, and 11.7 kyr BP, respectively. Each phase corresponds to a package of laminated silty clay containing sparse molluscs but abundant ostracods. Silty sand beds, indicative of a beach or swash zone, mark periods when the lake level dropped at this site. Ostracod assemblages are dominated by highly cosmopolitan genera. However, *Potamocypris*, indicative of a restricted local environment, dominated the top of the section. At the same

time, $\delta^{18}O$ analyses from ostracod shells show a shift toward fresher conditions beginning in the middle of Phase 2, which is interpreted to reflect an overflow connection into the Nile drainage system.

The timing of the initial highstand event at 13.9 kyr BP pushes back the earliest conclusive evidence for Lake Turkana's response to the AHP by over 1 kyr (Figure 5a). This corresponds well with records from the Ethiopian Highlands (Figure 5b) (Shanahan et al., 2015; Street-Perrott and Perrott, 1990), which also show increased lake levels at this time. This relationship fits the broader context of the basin as the Ethiopian Highlands are the dominant catchment sustaining Lake Turkana via the Omo River. In contrast, Lake Challa on the border between Tanzania and Kenya responded to the AHP with increased wetness around 15–14 kyr BP (Shanahan et al., 2015; Tierney et al., 2011), which precedes the Turkana Basin. The cessation of lacustrine deposition between Phase 2 and Phase 3 corresponds to the YD event at ~12.7 kyr BP, reflecting the regional trend of increased aridity across tropical Africa (Foerster et al., 2015; Talbot et al., 2007). The lake then quickly rebounded to fresh, overflow conditions by 11.7 kyr BP as indicated by the sedimentology, isotopic, and biological proxies. Locally, however, the area around Kabua Gorge became a restricted marshy environment that was resource rich for the human populations living in the vicinity. The close association between human populations and water resources during this time period is supported by archeological evidence of fishing from bone harpoons associated with fish fossils excavated from Galana Boi sediments around the basin (Barthelme, 1977, 1985; Robbins, 1975), including sites located in the region around Kabua Gorge (Beyin, 2011). Ultimately, understanding the transition into the AHP and the start of the Holocene in East Africa is essential for providing context for the Holocene stability and the dynamic cultural evolution, including early evidence of warfare (Mirazon Lahr et al., 2016), that accompanied it.

Acknowledgements

The authors are grateful for the field assistance of Francis Ekai of the Turkana Basin Institute (TBI); Ekeno John (Mac) Mark, formerly of TBI; and Dominic Ikai of Nariokotome.

Funding

The study was supported by Rutgers University Graduate School Special Study Dissertation Awards (2011 and 2012), Geological Society of America Student Research Grant, AAPG Marta S. Weeks Named Grant, and SEPM Student Research Grant.

Supplemental material

Supplemental material for this article is available online.

References

Barthelme JW (1977) Holocene sites north-east of Lake Turkana: A preliminary report. *Azania* 12(1): 33–41.

Barthelme JW (1985) *Fisher-Hunters and Neolithic Pastoralists in East Turkana, Kenya*. Oxford: British Archaeological Reports.

Beck CC (2015) *A multiproxy approach to deciphering terrestrial climate records from the Turkana Basin, Kenya*. PhD Thesis, Rutgers University.

Beck CC, Feibel CS, Wright JD et al. (2014) A multi-proxy approach to tracing a regressive event at Ferguson's Gulf, Lake Turkana, Kenya: Implications for modern analogues to assist in interpretations of the Plio-Pleistocene record. In: *European Geosciences Union Abstracts*, Vienna, 27 April–2 May.

Berke MA, Johnson TC, Werne JP et al. (2012) A mid-Holocene thermal maximum at the end of the African humid period. *Earth and Planetary Letters* 351–352: 95–104.

Berke MA, Johnson TC, Werne JP et al. (2014) Characterization of the last deglacial transition in tropical East Africa: Insights from Lake Albert. *Palaeogeography, Palaeoclimatology, Palaeoecology* 409: 1–8.

Beyin A (2011) Recent archaeological survey and excavation around the greater Kalokol area, west side of Lake Turkana: Preliminary findings. *Nyame Akuma* 75: 40–50.

Bloszies C, Forman SL and Wright DK (2015) Water level history for Lake Turkana, Kenya in the past 15,000 years and a variable transition from the African humid period to Holocene aridity. *Global and Planetary Change* 132: 64–76.

Brown DS (1980) *Freshwater Snails of Africa and Their Medical Importance*. London: Taylor & Francis.

Brown FH and Fuller CR (2008) Stratigraphy and tephra of the Kibish Formation, southwestern Ethiopia. *Journal of Human Evolution* 55(3): 366–403.

Butzer KW, Isaac GL, Richardson JL et al. (1972) Radiocarbon dating of East African lake levels. *Science* 175(4027): 1069–1076.

Carbonel P and Peypouquet J-P (1979) Les ostracodes des series du Bassin de I'Omo. *Bulletin de l'Institut de géologie du Bassin d'Aquitaine* 25: 167–199.

Cohen A (1986) Distribution and faunal associations of benthis invertebrates at Lake Turkana, Kenya. *Hydrobiologia* 141: 179–197.

Cohen A, Campisano C, Arrowsmith R et al. (2016) The Hominin Sites and Paleolakes Drilling Project: inferring the environmental context of human evolution from eastern Africa rift lake deposits. *Scientific Drilling* 21: 1–16.

deMenocal PB (1995) Plio-Pleistocene African climate. *Science* 270: 53–59.

deMenocal PB, Ortiz J, Guilderson TP et al. (2000) Arupt onset and termination of the African humid period: Rapid climate responses to gradual insolation forcing. *Quaternary Science Reviews* 19: 347–361.

Feibel CS (1988) *Paleoenvironments of the Koobi Fora Formation, Turkana Basin, Northern Kenya*. PhD Thesis, University of Utah.

Feibel CS (2011) A geological history of the Turkana Basin. *Evolutionary Anthropology* 20(6): 206–216.

Foerster V, Junginger A, Langkamp O et al. (2012) Climatic change recorded in the sediments of the Chew Bahir basin, southern Ethiopia, during the last 45,000 years. *Quaternary International* 274: 25–37.

Foerster V, Vogelsang R, Junginger A et al. (2015) Environmental change and human occupation of southern Ethiopia and northern Kenya during the last 20,000 years. *Quaternary Science Reviews* 129: 333–340.

Garcin Y, Junginger A, Melnick D et al. (2009) Late Pleistocene–Holocene rise and collapse of Lake Suguta, northern Kenya Rift. *Quaternary Science Reviews* 28: 911–925.

Garcin Y, Melnick D, Strecker MR et al. (2012) East African mid-Holocene wet–dry transition recorded in palaeo-shorelines of Lake Turkana, northern Kenya Rift. *Earth and Planetary Science Letters* 331–332: 322–334.

Halfman JD, Johnson TC and Finney BP (1994) New AMS dates, stratigraphic correlations and decadal climatic cycles for the past 4 Ka at Lake Turkana, Kenya. *Palaeogeography, Palaeo-Climatology, Palaeoecology* 111: 83–98.

Harmand S, Lewis JE, Feibel CS et al. (2015) 3.3-million-year-old stone tools from Lomekwi 3, West Turkana, Kenya. *Nature* 521(7552): 310–315.

Harvey CPD and Grove T (1982) A prehistoric source of the Nile. *The Geographical Journal* 148(3): 327–336.

Junginger A and Trauth MH (2013) Hydrological constraints of paleo-Lake Suguta in the Northern Kenya Rift during the African humid period (15–5kaBP). *Global and Planetary Change* 111: 174–188.

Junginger A, Roller S, Olaka LA et al. (2014) The effects of solar irradiation changes on the migration of the Congo Air Boundary and water levels of paleo-Lake Suguta, Northern Kenya Rift, during the African humid period (15–5ka BP). *Palaeogeography, Palaeoclimatology, Palaeoecology* 396: 1–16.

Kutzbach JE and Liu Z (1997) Response of the African monsoon to orbital forcing and ocean feedbacks in the middle Holocene. *Science* 278: 440–443.

Li H-C and Ku T-L (1997) δ13C-δ18O covariance as a paleohydrological indicator for closed-basin lakes. *Palaeogeography, Palaeoclimatology, Palaeoecology* 133: 69–80.

Martin RL (2014) *Late quaternary sedimentary geology of North Turkwel, Turkana County, Kenya*. Masters Thesis, Rutgers University.

Melnick D, Garcin Y, Quinteros J et al. (2012) Steady rifting in northern Kenya inferred from deformed Holocene lake shorelines of the Suguta and Turkana basins. *Earth and Planetary Science Letters* 331–332: 335–346.

Mirazon Lahr M, Rivera F, Power RK et al. (2016) Inter-group violence among early Holocene hunter-gatherers of West Turkana, Kenya. *Nature* 529(7586): 394–398.

Morrissey A and Scholz CA (2014) Paleohydrology of Lake Turkana and its influence on the Nile River system. *Palaeogeography, Palaeoclimatology, Palaeoecology* 403: 88–100.

Nicholson SE (1996) A review of climate dynamics and climate variability in Eastern Africa. In: Johnson TC and Odada EO (eds) *The Limnology, Climatology and Paleoclimatology of the East African Lakes*. Amsterdam: Gordon and Breach Publishers, pp. 25–56.

O'Neil JR, Clayton RN and Mayeda TK (1969) Oxygen isotope fractionation in divalent metal carbonates. *Journal of Chemical Physics* 51: 5547–5558.

Owen RB and Renaut RW (1986) Sedimentology, stratigraphy and palaeoenvironments of the Holocene Galana Boi Formation, NE Lake Turkana, Kenya. In: Frostick LE, Renaut RW, Reid I et al. (eds) *Sedimentation in the African Rifts (Geological Society Special Publications)*. Oxford: *Blackwell Scientific Publications*, pp. 311–322.

Owen RB, Barthelme JW, Renaut RW et al. (1982) Palaeolimnology and archaeology of Holocene deposits north-east of Lake Turkana, Kenya. *Nature* 298: 523–528.

Rasmussen SO, Andersen KK, Svensson AM et al. (2006) A new Greenland ice core chronology for the last glacial termination. *Journal of Geophysical Research* 111: D06102.

Ricketts RD and Anderson RF (1998) A direct comparison between the historical record of lake level and the δ18O signal in carbonate sediments from Lake Turkana, Kenya. *Limnology and Oceanography* 43(5): 811–822.

Robbins LH (1975) Bone artefacts from the Lake Rudolf Basin, East Africa. *Current Anthropology* 16: 632–633.

Russell JM, Verschuren D and Eggermont H (2007) Spatial complexity of Little Ice Age climate in East Africa: Sedimentary records from two crater lake basins in Western Uganda. *The Holocene* 17(2): 183–193.

Shanahan TM, McKay NP, Hughen KA et al. (2015) The time-transgressive termination of the African humid period. *Nature Geoscience* 8(2): 140–144.

Shea JJ and Hildebrand EA (2010) The Middle Stone Age of West Turkana, Kenya. *Journal of Field Archaeology* 35(4): 355–364.

Stager JC, Ryves DB, Chase BM et al. (2011) Catastrophic drought in the Afro-Asian monsoon region during Heinrich event 1. *Science* 331: 1299–1302.

Street-Perrott FA and Perrott RA (1990) Abrupt climate fluctuations in the tropics: The incluence of Atlantic Ocean circulation. *Nature* 343: 607–612.

Talbot MR, Filippi ML, Jensen NB et al. (2007) An abrupt change in the African monsoon at the end of the Younger Dryas. *Geochemistry, Geophysics, Geosystems* 8: Q03005.

Tierney JE and deMenocal PB (2013) Abrupt shifts in Horn of Africa hydroclimate since the last glacial maximum. *Science* 342: 843–846.

Tierney JE, Russell JM, Sinninghe Damsté JS et al. (2011) Late quaternary behavior of the East African monsoon and the importance of the Congo Air Boundary. *Quaternary Science Reviews* 30(7–8): 798–807.

van der Lubbe HJL, Krause-Nehring J, Junginger A et al. (2017) Gradual or abrupt? Changes in water source of Lake Turkana (Kenya) during the African humid period inferred from Sr isotope ratios. *Quaternary Science Reviews* 174: 1–12.

Vondra CF, Johnson GD, Bowen GE et al. (1971) Preliminary stratigraphical studies of the East Rudolf Basin, Kenya. *Nature* 231: 245–248.

Vonhof HB, Joordens JCA, Noback ML et al. (2013) Environmental and climatic control on seasonal stable isotope variation of freshwater molluscan bivalves in the Turkana Basin (Kenya). *Palaeogeography, Palaeoclimatology, Palaeoecology* 383–384: 16–26.

Whitworth T (1965) The pleistocene lake beds of Kabua, Northern Kenya. *Durham University Journal* 57: 88–100.

Wood B and Leakey M (2011) The Omo-Turkana Basin fossil hominins and their contribution to our understanding of human evolution in Africa. *Evolutionary Anthropology* 20(6): 264–292.

Yuretich RF and Cerling TE (1983) Hydrogeochemistry of Lake Turkana, Kenya: Mass balance and mineral reactions in an alkaline lake. *Geochimica et Cosmochimica Acta* 47: 1099–1109.

Zhai D, Xiao J, Fan J et al. (2014) Differential transport and preservation of the instars of Limnocythere inopinata (Crustacea, Ostracoda) in three large brackish lakes in northern China. *Hydrobiologia* 747(1): 1–18.